Archives of Biochemistry and Biophysics 771 (2025) 110526

Contents lists available at ScienceDirect

Archives of Biochemistry and Biophysics

journal homepage: www.elsevier.com/locate/yabbi

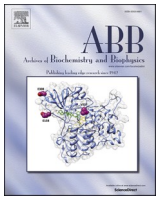

Preserving antimicrobial efficacy while extending peptide longevity: effects of residue glycosylation

Ilaria Di Donato [a,2], Attila Tortorella [a,b,2], Marco Campanile [a], Andreas Rumpel [c,1], Linda Leone [a], Andrea Bosso [d], Luigi Petraccone [a], Angelina Lombardi [a], Roland Winter [c], Pompea Del Vecchio [a,*], Rosario Oliva [a,**]

[a] Department of Chemical Sciences, University of Naples Federico II, Via Cintia 26, 80126, Naples, Italy
[b] Scuola Superiore Meridionale (SSM), Via Mezzocannone 4, Naples, Italy
[c] Faculty of Chemistry and Chemical Biology, Biophysical Chemistry, TU Dortmund University, Otto-Hahn-Str. 4a, 44227, Dortmund, Germany
[d] Department of Biology, University of Naples Federico II, Via Cintia 26, 80126, Naples, Italy

A B S T R A C T

The spread of antibiotic-resistant bacteria has prompted the search for new drugs. Antimicrobial peptides (AMPs) are promising candidates, but their pharmacological application is limited by their poor stability, especially against proteolytic enzymes. A strategy to increase AMPs half-life is the introduction of sugars at key residues, a process termed glycosylation. In this work, the RLK10 peptide was obtained from the GKY10 peptide, by replacing the glutamine residue with an asparagine. Then, it was glycosylated at the asparagine by introducing a N-acetylglucosamine, obtaining the peptide RLK10-NAG. To further increase the stability, the N-terminus was acetylated, producing the Ac-RLK10-NAG peptide. *In cellulo* assays revealed that RLK10 modifications limitedly affect its antimicrobial activity. However, using POPE/POPG liposomes as a bacterial model membrane, marked differences in their mode of action were found. Stability tests against proteases revealed that the N-acetylglucosamine significantly enhances the stability of the RLK10 sequence. Unexpectedly, the acetylation didn't improve the peptide resistance against proteases, rather it increased its degradation susceptibility. These results demonstrate that glycosylation is an effective strategy to improve the AMPs stability while marginally affecting their biological activity, opening to the possibility of using AMPs in medicine and extending their use into other areas such as food preservation.

1. Introduction

The increasing spread of bacteria resistant to conventional antibiotics is one of the major concerns worldwide [1]. As pointed out by the World Health Organization (WHO), bacterial resistance is responsible for millions of deaths every year and leads to a significant increase of healthcare costs [1]. It is estimated that the number of deaths will rise to around 10 million per year by 2050 [2]. The spread of resistant bacterial strains is mainly due to the misuse and abuse of antibiotics in humans, animals and plants [1,3]. Bacteria have developed different strategies to inactivate antibiotics and survive their exposure. For example, bacteria can modify antibiotics through enzyme-promoted reactions (*e.g.,* phosphorylation, acetylation), thus altering their binding capability to the target [4,5]. Another strategy is the enzymatic degradation of antibiotics, as exemplified by β-lactamases, a class of enzymes that inactivate β-lactams (penicillin) [6]. Another remarkable example of such a strategy is the hydrolysis of β-lactams mediated by alpha phenol-soluble modulins (PSMαs), functional amyloids found in the biofilm of *S. aureus* [7]. Moreover, bacteria can prevent the accumulation of antibiotics inside their cells by acting on their membrane proteins. For example, in β-lactams-resistant *P. aeruginosa*, the decrease of the number of porins in the outer membrane leads to a significant decrease of antibiotic influx [4]. Therefore, new antibiotics that can circumvent this problem are urgently needed, and the efforts of the scientific community are devoted to the search and development of new and more effective antimicrobial drugs. A promising class of compounds is represented by antimicrobial peptides (AMPs). AMPs are short, usually cationic peptides exhibiting antimicrobial activity against bacteria,

* Corresponding author.
** Corresponding author.
E-mail addresses: pompea.delvecchio@unina.it (P. Del Vecchio), rosario.oliva2@unina.it (R. Oliva).
[1] Present address: Institute of Chemistry, Membrane Biophysics and NMR, University of Strasbourg/CNRS, UMR7177, Rue Blaise Pascal 1, 67000, Strasbourg, France.
[2] These authors contributed equally to this work.

https://doi.org/10.1016/j.abb.2025.110526
Received 12 May 2025; Received in revised form 28 June 2025; Accepted 29 June 2025
Available online 1 July 2025

fungi, parasites, virus and even cancer cells [8,9]. They are part of the innate immune systems of almost all forms of life and are at the forefront fighting the invasion of harmful microorganisms. Although AMPs play various roles (*e.g.,* in wound healing), they are primarily known for their antibacterial activity. This important function is carried out through the selective interaction of cationic peptides with the bacterial membrane, which has a high fraction of negatively charged lipids (*e.g.,* phosphatidylglycerols and cardiolipins). Upon interaction, AMPs can induce permanent damages to the membrane, drastically altering the viability of the cell and leading to its death [10]. Some models have been developed to explain the action mechanism of AMPs (*e.g.,* barrel-stave, toroidal, carpet, domain formation, etc.) [11]. However, it is challenging to describe a given peptide activity relying on a single mechanism, and often AMPs act through a combination of two or more "classic" modes of action. The exact way through which a peptide acts, depends on the physico-chemical properties of the peptide itself (*e.g.,* charge, hydrophobicity) and of the membrane (its lipid composition, phase, fluidity, hydration level) [12]. The interaction is usually not receptor-mediated, and this aspect may be responsible for the low propensity of bacteria to develop resistance to AMPs [13,14]. In addition, some AMPs can have intracellular targets (proteins and nucleic acids) that are involved in fundamental biochemical reactions and can gain access to the cytosol of the cell without damaging the membrane [11,15]. Indeed, it has been shown that AMPs can be used to target intracellular biocondensates, such as the ones formed by α-synuclein involved in Alzheimer's disease [16] and by the nucleocapsid protein and RNA during viral infection operated by SARS-CoV-2 [17].

Although AMPs show great potential as antibiotics, their direct application is hampered by several problems that need to be addressed. The stability of AMPs depends on temperature, pH and exposure to UV radiation causing residues oxidation. Of note, once AMPs are administered, they are easily hydrolysed by proteases present in the human body or secreted by bacteria at the site of infection, resulting in the fragmentation and deactivation of the peptides [18]. Various strategies have been developed to address this problem (Fig. 1), such as the introduction of unnatural amino acids [19], D-enantiomers [20] or by designing N-substituted glycine oligomers (peptoids) [21]. which render AMPs unrecognizable by endopeptidases and by protecting peptide termini by exopeptidases for example through the carboxylation of the N-terminus and/or the amidation of the C-terminus [20]. Other strategies include a covalent link of fatty acids (producing lipopeptides) and PEG (a process known as PEGylation), the encapsulation in nanoparticles (*e.g.* or cyclodextrins [22,23].

An alternative approach is the glycosylation of peptides at key residues. Glycosylation is ubiquitous in nature and many proteins are subjected to this process during post-translational modification [24]. Indeed, some AMPs are naturally glycosylated, for example, formacein 1 isolated from the ant *Myrmecia gulosa* has an O-linked N-acetylgalactosamine at the Thr residue [25]. The glycosylation can occur at four different residues [24]: at the Asn residue leading to N-glycosylation, at Ser, Thr and Tyr residues producing O-glycosylated proteins, and glycosylation of Trp and free Cys leading to the C-glycosylated and S-glycosylated proteins, respectively. Glycosylation of key residues of AMPs can have a strong impact on their antimicrobial activity [25]. For example, in the case of formacein 1, removal of the sugar moiety results in a marked decrease in antimicrobial activity, highlighting the key role of the saccharide [25]. Glycosylation can also play a prominent role in increasing the stability of peptides against proteases [24]. For example, glycosylation of LL-III was shown to significantly reduce the susceptibility of the peptide to proteases while not altering its antibacterial activity [26].

In this work, starting from the previously characterized peptide GKY10 (RLKKWI**Q**KVI) [27], the peptide RLK10 (RLKKWI**N**KVI) was obtained by replacing a glutamine residue with an asparagine. The sugar β-D-(Acetylamino)-2-deoxy-glucopyranose (also named N-acetylglucosamine, abbreviated as NAG) was introduced at the Asn residue of the AMP RLK10, producing an N-glycosylated form of the peptide (RLK10-NAG). Next, RLK10-NAG was acetylated, giving the double-modified peptide Ac-RLK10-NAG. The interaction of the two peptides with bacterial model membranes was studied in detail and compared to the unmodified form RLK10. In addition, the antibacterial activity of the peptides was evaluated by determining the MIC (minimal inhibitory concentration) values against a panel of both *Gram-negative* and *Gram-positive* bacterial strains. Finally, the stability of the peptides against the enzymes α-chymotrypsin and pepsin was assessed *in vitro* and on the viability of bacteria by incubating the peptides with the enzyme and then administering them to the bacteria.

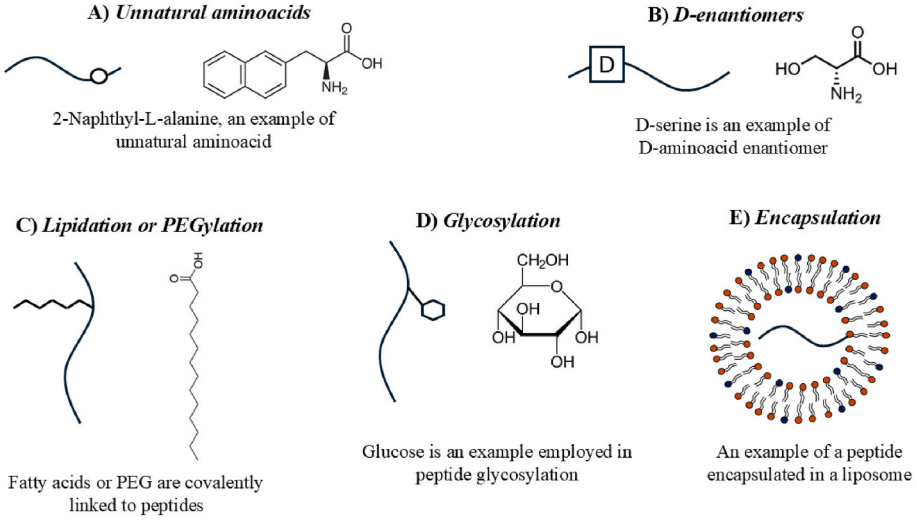

Fig. 1. Some strategies adopted to increase the resistance of AMPs to the hydrolysis mediated by proteolytic enzymes. Introduction of (A) unnatural amino acids and (B) D-enantiomers in the primary sequences of peptides. Peptide lipidation or PEGylation (C): the first refers to the introduction of a fatty acid moiety, the second to the addition of polyethylene glycol (PEG) chains. Peptide glycosylation at key residues (D), the modification used in this study. Peptide encapsulation in nanostructures (*e.g.*, liposomes, nanoparticles).

2. Materials and Methods

2.1. Materials

Peptides were chemically synthesized by solid phase peptide synthesis (SPPS) and purified by reverse-phase HPLC (RP-HPLC). All Fmoc-protected amino acids as well as the resin and the coupling reagent 1-[Bis(dimethylamino)methylene]-1H-1,2,3-triazolo [4,5-b]pyridinium 3-oxide hexafluorophosphate (HATU) were purchased from Novabiochem (Merck). N,N-diisopropylethylamine (DIEA) and triisopropylsilane (TIS) were purchased from Sigma-Aldrich. Piperidine, trifluoroacetic acid (TFA) and all solvents used in the synthesis and purification were supplied by Romil. The coupling reagent 1-hydroxybenzotriazole (HOBt) was purchased from Anaspec. The lipids 1-palmitoyl-2-oleoyl-*sn*-glycero-3-phosphoethanolamine (POPE), 1-palmitoyl-2-oleoyl-*sn*-glycero-3-phospho-(1′-rac-glycerol) (sodium salt) (POPG) were purchased from Avanti Polar Lipids Inc. (Alabaster, AL, USA) and used without further purification. The chloroform, methanol, ethanol and dimethyl sulfoxide (DMSO) solvents were purchased from Sigma Aldrich Chemical. The fluorescent probe Laurdan (6-dodecanoyl-N,N-dimethyl-2-naphtylamine) was purchased from Sigma Aldrich. Sample preparations for the biophysical experiments were prepared in 10 mM phosphate buffer solution at pH 7.4.

2.2. Peptides synthesis

Peptides were assembled stepwise using an ABI 433A peptide synthesizer (Applied Biosystems, Foster City, CA, USA) on a 0.05 mmol scale. The acid labile Fmoc-Ile-NovaSyn TGA resin (0.20 mmol/g as loading), preloaded with Ile, was used as solid support. Standard Fmoc protocols were used for deprotection, activation, coupling and capping cycles. Amino acids were activated in situ with an equimolar amount of HATU as the coupling reagent. A 10-fold excess of amino acid with respect to the synthesis scale was used in each coupling. To improve yields, a double coupling procedure was applied to each amino acid except the glycosylated asparagine (Fmoc-L-Asn((Ac)3-β-D-GlcNAc)-OH), for which a single coupling was performed with 7-fold excess of amino acid. For Ac-RLK10 and Ac-RLK10-NAG peptides, the final acetylation step was performed using a solution of acetic anhydride, DIEA and HOBt in N-methylpyrrolidone (NMP). After synthesis completion, the resin was washed with N,N-dimethylformamide (DMF), dichloromethane (DCM) and diethyl ether and finally dried. Cleavage of peptides from the resin with concomitant sidechain deprotection was achieved by treatment with a solution of TFA:TIS:H_2O (95:2.5:2.5, v/v/v). The reaction was carried out under magnetic stirring at 0 °C for 1 h, followed by 1 h at room temperature. The TIS acted as a scavenger of free radicals and of carbocations that are released during the removal of the sidechains protecting groups. All peptides were obtained with the free carboxylic group at the C-terminus upon cleavage, thanks to the presence of 4-hydroxymethylphenoxyacetic acid linker on the resin support. After cleavage, the resin was filtered under vacuum and the solution was concentrated to a small volume. The crude peptides were then precipitated by adding an excess of cold diethyl ether and centrifuged at 4000 rpm for 10 min. The supernatant was then discarded and the precipitate washed 3 times with fresh diethyl ether. The peptides were dried under reduced pressure, re-dissolved in H_2O 0.1 % TFA and lyophilized.

2.3. Peptide purification

The crude peptides were dissolved in a small volume of H_2O 0.1 % TFA and purified by reverse – phase high pressure liquid chromatography (RP-HPLC) using a Shimadzu LC-8A preparative HPLC system (Shimadzu, Kyoto, Japan), equipped with an SPD-M10 AV UV/Vis detector. A Vydac C18 column (250 mm × 22 mm; 10 μm) was eluted with a linear gradient of H_2O 0.1 % TFA (eluent A) and acetonitrile 0.1 % TFA (eluent B), at 23 mL/min. A gradient from 10 to 60 % B over 50 min was used for all purifications. All the collected fractions were analyzed for purity by using a Shimadzu LC-10ADvp analytical HPLC equipped with an SPDM10Avp diode-array detector. A Vydac C18 column (150 mm × 4.6 mm, 5 μm) was used in all analyses, eluted with the same gradient used for purification, over 30 min at a flowrate of 1 mL/min (see Figures S1, S2 and S3 for RP-HPLC chromatograms of peptides). Peptide identity was ascertained by electrospray ionisation mass spectrometry (ESI-MS) analyses, performed on a Shimadzu LC-MS-2010EV system with ESI interface and a quadrupole mass analyzer. Mass spectra were acquired in the positive ion scanning mode in the 500–1500 range of *m/z* (Figures S4, S5 and S6).

2.4. N-acetylglucosamine deprotection and desalting

Removal of the acetyl groups from protected hydroxyls of N-acetylglucosamine (NAG) was achieved by treating the pure glycosylated peptides (1.5 mM) with a solution of sodium methoxide in methanol (8 mg/mL) at pH 9. For both peptides, the reaction was performed overnight at room temperature under magnetic stirring. Complete deprotection was assessed by RP-HPLC and MS analysis. A shift towards lower retention times was observed upon sugar deprotection due to the greater hydrophilicity of the deprotected peptides compared to the precursors. The reaction solutions were then neutralized by treatment with a solution of 1 % CH_3COOH in MeOH and then evaporated to dryness. The resulting peptides were solubilized in H_2O 0.1 % TFA and lyophilized. Subsequently, the peptides were purified from excess acetate salts by reverse phase flash chromatography. This desalting procedure was carried out using a Biotage® Isolera system with a Sfär Bio C4 D Duo 300 Å 20 μm 10 g column, eluted with a linear gradient of H_2O 0.1 % TFA (solvent A) and acetonitrile 0.1 % TFA (solvent B), from 0 to 60 % B over 10 column volumes at a flowrate of 25 mL/min.

2.5. Anionic exchange

The trifluoroacetate counterion was removed from the synthesized peptides by anionic exchange with chloride. The pure peptides (1 mg/mL) were dissolved in 10 mM HCl, then frozen and lyophilized after 5 min incubation. The procedure was repeated twice. Complete removal of TFA was assessed by ^{19}F NMR.

2.6. Liposome preparation

Vesicles composed of POPE/POPG (7:3 mol/mol) phospholipids were selected as a model bacterial membrane and prepared using the thin-film hydration method, as previously described [28]. Lipid films were hydrated using a 10 mM sodium phosphate solution, pH 7.4. Multilamellar vesicles (MLVs) were used for DSC experiments, while 100 nm unilamellar vesicles (LUVs) were utilized for spectroscopic experiments. LUVs were prepared by extrusion through polycarbonate filters using a mini extruder from Avanti Polar Lipids Inc. (Alabaster, AL, USA) equipped with two 1.0 mL Hamilton syringes (Hamilton, Reno, NV, USA). Dynamic light scattering (DLS) measurements were performed to confirm the vesicle size. Liposome samples containing peptides were prepared by mixing appropriate amounts of peptide solution and liposomes to achieve the desired lipid-to-peptide (L/P) ratio.

2.7. Circular dichroism spectroscopy (CD)

Far-UV CD measurements were performed using a Jasco J-1500 Spectropolarimeter (Jasco Analytical Instruments, Tokyo, Japan). Spectra were recorded in the wavelength range of 190–260 nm using a 0.1 cm pathlength quartz cuvette under the following experimental conditions: 0.5 nm resolution, 50 nm/min scanning speed, 4 nm bandwidth and 2 s integration time. The temperature was set to 25 °C. Each spectrum represents the average of five accumulations and the ellipticity normalized per mole of residue. Peptide samples were prepared in 10

mM sodium phosphate buffer at the concentration of 30 μM both in the absence and presence of POPE/POPG large unilamellar vesicles (LUVs) at a total lipid concentration of 1.5 mM (L/P ratio of 50). Background signals were subtracted for all samples. The percentages of helical content (H_C) for all peptides were estimated using the following equation: $H_C = [\theta]^{obs}_{222} / \left[-40000 \cdot \left(1 - \frac{2.5}{n}\right)\right]$ where $[\theta]^{obs}_{222}$ is the observed molar ellipticity at 222 nm and n is the number of the residues [29].

2.7.1. Differential scanning calorimetry (DSC)

DSC measurements were performed by means of a high sensitivity Nano DSC (TA Instruments, New Castle, DE, USA) equipped with 300 μL twin gold capillary cells, pressurized to 3 atm. For all DSC experiments, samples of POPE/POPG multilamellar vesicles (MLVs) were analyzed both in the absence and presence of peptides in 10 mM sodium phosphate buffer at pH 7.4. Each sample was scanned from 20 to 55 °C at least four times, using a scanning rate of 1 °C/min. Superimposition of successive heating and cooling scans confirmed the reversibility of the process. The excess heat capacity function ($<\Delta C_p>$) was obtained after baseline subtraction. Buffer-buffer scans were recorded under the same conditions and subtracted from sample profiles. Data analysis was performed by using the *Nano Analyze* software provided by the manufacturer and plotted using the Origin software package (OriginLab, Northampton, MA, USA).

2.8. Fluorescence spectroscopy

Fluorescence experiments were performed on a Fluoromax-4 (Horiba, Edison, NJ, USA) operating in the steady state mode at the temperature of 25 °C. Peptide solutions and liposome suspensions were prepared in 10 mM sodium phosphate buffer at pH 7.4.

2.8.1. Binding experiments

The interaction of peptide with liposomes was investigated by recording the fluorescence emission spectra of the Trp-containing peptides at increasing POPE/POPG vesicle concentration. The peptide concentration was fixed at 7.6 μM, while the total lipid concentration ranged between 0 and 1 mM. Emission spectra were recorded between 300 nm and 470 nm after excitation at 280 nm. The binding isotherms were obtained by plotting the relative fluorescence intensities (F/F_0) at 344 nm as a function of lipid concentration, where F_0 and F is the fluorescence intensity of the peptide in the absence and presence of vesicles, respectively. To minimize liposomes-induced light scattering, the experiments were performed by setting the excitation and the emission polarizers at 90° and 0°, respectively. The reported data were analyzed to calculate the mole fraction partition constant (K_x) according to the method described by Ladokhin [30].

2.8.2. Laurdan fluorescence emission spectra and GP calculation

Laurdan fluorescence emission spectra were recorded in the 360–650 nm range using an excitation wavelength of 340 nm. Both slits for the excitation and emission monochromators were set to 7 nm. Measurements were performed in a 1 cm path length cuvette. The total lipid concentration was fixed at 50 μM, while the peptide concentration was varied between 0 and 50 μM. The Laurdan concentration was 1.5 μM. Laurdan generalized polarization (*GP*) was calculated according to the relation $GP = (I_{440}–I_{490})/(I_{440}+I_{490})$, where I_{440} and I_{490} are the fluorescence intensities at 440 and 490 nm, respectively [31].

2.8.3. Fluorescence kinetics

Fluorescence kinetics experiments were performed to evaluate the efficacy of the peptide modifications on its resistance to enzymatic cleavage. To this end the substrate AAF-AMC and the enzymes α-chymotrypsin and pepsin were used. The concentration of each peptide was fixed at 50 μM, the substrate AAF-AMC at 80 μM, and α-chymotrypsin and pepsin at 10 nM and 5 μM, respectively. The substrate AAF-AMC was dissolved in DMSO. The stock solution of α-chymotrypsin was prepared in phosphate buffer at pH 7.4 and the concentrations were evaluated as previously described by us [32]. The pepsin stock solution was prepared in acetate buffer at pH 4.0 and its concentration was evaluated spectrophotometrically using a molar extinction coefficient of 49650 cm^{-1} M^{-1} [33]. The experiments were performed in a 0.3 cm pathlength cuvette, monitoring the fluorescence intensity at 460 nm with slits for the excitation and emission monochromators set to 7 nm.

2.9. RP-HPLC evaluation of peptides hydrolysis mediated by proteolytic enzymes

To assess the peptides' stability to proteases 400 μM solutions of RLK10, RLK10-NAG or Ac-RLK10-NAG were incubated either with α-chymotrypsin (100 nM) for 15 min or with pepsin (200 nM) for 60 min. Reactions with α-chymotrypsin were performed in 50 mM phosphate buffer at pH 7.2, while reactions with pepsin were performed in 50 mM acetate buffer at pH 4.0. All reactions were carried out at room temperature under magnetic stirring. For each reaction, an aliquot of reaction mixture was taken and analyzed by RP-HPLC before the addition of the enzyme. Then, after the specified reaction times, the enzyme was separated from the reaction mixture by centrifugal filtration at 10000 rpm for 15 min using Amicon Ultra Centrifugal Filters with 10 kDa MWCO (Merck Millipore). The solution eluted from the filter was analyzed by RP-HPLC. All the RP-HPLC analyses were performed using a Vydac C18 column (150 mm × 4.6 mm, 5 μm), eluted with a linear gradient of H_2O 0.1 % TFA (eluent A) and acetonitrile 0.1 % TFA (eluent B). Specifically, a gradient from 10 to 50 % B over 20 min and following from 50 % to 90 % B over 15 min was used at a flowrate of 1 mL/min.

To estimate the amount of intact peptide following protease treatment, the percentage peak area corresponding to the peptide was measured by integration of the chromatographic trace at 210 nm.

2.10. Biological assays

2.10.1. Antimicrobial activity and serum stability

The antimicrobial activity of GKY10 and RLK10 derived peptides was tested against *Acinetobacter baumannii* ATCC 17878, *Escherichia coli* ATCC 25922, *Staphylococcus aureus* ATCC 6538P and *Listeria monocytogenes* ATCC 7644 according to the broth microdilution method as previously described [27,34]. Briefly, bacteria were grown to mid-logarithmic phase in Luria Bertani broth (LB) at 37 °C. Cells were then diluted to 1×10^6 CFU/mL in Difco 0.5X Nutrient Broth (Becton-Dickenson, Franklin Lakes, NJ) containing increasing amounts of peptide. Following over-night incubation, MIC_{100} values were determined as the lowest peptide concentration needed for non-visible bacterial growth. To determine the peptides' protease stability [26], a 400 μM solution of RLK10 derived peptides were incubated with 100 nM α-chymotrypsin for 15 min at 37 °C or 200 nM pepsin for 60 min, and the antimicrobial activity was determined as described above against two bacterial strains. The peptide solution without proteases was used as control group. Finally, to determine peptides' serum stability, a 400 μM solution of each RLK10 derived peptides was incubated with 10 % fetal bovine serum (FBS) for 1 and 24 h at 37 °C, and then the antimicrobial activity was determined as described above.

3. Results

3.1. Modification of RLK10 peptide

In a previous study, the action mechanism of the peptide GKY20 (GKYGFYTHVFRLKKWIQKVI) derived from the human thrombin was characterized in detail [35]. It was shown that the region mainly responsible for its membrane-perturbation activity corresponds to its C-terminus decapeptide RLKKWIQKVI (GKY10, Table 1) [27]. This

Table 1
Sequence, charge and theoretical molecular weight of the peptides.

Peptide	Sequence[a]	Charge[b]	Molecular Weight[c]
GKY10	RLKKWI**Q**KVI	+4	1311.66
RLK10	RLKKWI**N**KVI	+4	1296.84
RLK10-NAG	RLKKWI**N(NAG)**KVI	+4	1499.93
Ac-RLK10-NAG	Ac-RLKKWI**N(NAG)**KVI	+3	1668.40

[a] NAG = N-acetylglucosamine.
[b] At pH = 7.4.
[c] In g mol^{-1}.

sequence was found to be active against both *Gram-positive* and *Gram--negative* bacteria [27]. Starting from this truncated form, it was introduced a point mutation replacing the glutamine (Q) in position 7 with an asparagine (N) residue, leading to the new sequence RLKKWINKVI, thus introducing a glycosylation site in its C-terminus portion. This substitution was motivated by the observation that in nature only the asparagine residue is a N-glycosylation site in proteins [24]. Further, the asparagine functionalized with NAG is commercially available at high purity, simplifying the synthetic procedure. In this way, the peptide RLK10-NAG was obtained (Table 1). It is expected that the presence of the sugar in proximity of the C-terminus offers a protection of that part of the sequence, disfavouring binding events and the hydrolysis of amide bonds mediated by proteolytic enzymes. Finally, the glycosylated peptide was further modified by acetylating the terminal-free amino group. This modification was introduced for two reasons: i) to protect the N-terminal region from proteolytic events and ii) to N-cap the N-terminus, thus increasing the propensity of the peptide to adopt a helical structure, which is an important factor in determining the biological activity and action mechanism of linear cationic peptides [36,37]. The structures of all RLK10 derivatives are reported in Fig. S7.

3.2. Biological assays

3.2.1. Evaluation of the miminum inhibitory concentration (MIC)

To evaluate the antimicrobial activity of RLK10 and its analogues, measurements of the minimum inhibitory concentrations (MIC) were carried out on both *Gram-positive* and *Gram-negative* bacterial strains. As a control, the same experiments were also carried out with the peptide GKY10. The results are reported in Table 2 and show that the Q → N (GKY10 → RLK10) substitution alone did not result in any alteration of the MIC values. This is an expected result as the Q and N residues have similar physico-chemical properties. The presence of NAG confers a slight increase in the MIC values against *E. coli* and *S. aureus,* still preserving a powerful antimicrobial activity (12.5 μM). The MIC value increased to 25 μM in the case of *L. monocytogenes* and a further increase was observed for *A. baumannii*. When the acetylation and glycosylation modifications are combined, the antimicrobial activity of RLK10 is significantly altered, but not suppressed. Summarizing the data reported in Table 2, it can be concluded that RLK10 generally has the highest antimicrobial potency, followed by RLK10-NAG and finally Ac-RLK10-NAG.

3.3. Stability in serum and against proteases

To evaluate the proteolytic stability of RLK10 and its modified forms, the antimicrobial activities of all peptides were analyzed after the treatment with α-chymotrypsin (α-CT) or pepsin. The enzyme α-CT is part of the mammalian digestive environment and is capable to hydrolyze the amide bond at the C-terminus of aromatic (Trp, Tyr and Phe) and Leu residues [32,38,39]. Thus, two cleavages are possible in the primary sequence of RLK10 peptides: at the bond between residues 2 and 3 and at the amide bond between residues 5 and 6 (Fig. 2). Pepsin, on the other hand, is a proteolytic enzyme whose cutting site depends on the adjacent residue [39–41]. In the present case, pepsin at pH 4.0 can cleave the bonds between residues 2 and 3, and between residues 4 and 5 (Fig. 2).

In brief, the peptides were treated with α-CT or pepsin; subsequently, the treated peptides were administered to two different bacterial strains, *Escherichia coli* ATCC 25922, a *Gram-negative* strain, and *Staphylococcus aureus* ATCC 6538P, a *Gram-positive* strain and the MIC values were determined. The data on the antimicrobial activities are listed in Table 3. The treatment of peptide RLK10 with α-CT completely abolished its antimicrobial activity against both bacterial strains, as the MIC values were >200 μM. The same result was obtained for Ac-RLK10-NAG. It is noteworthy that the stability of the peptide is maintained exclusively in

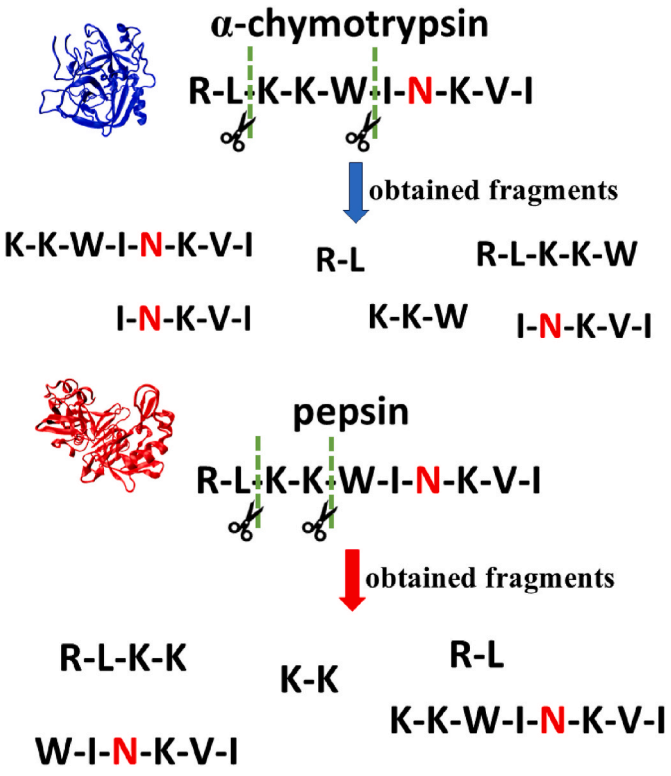

Fig. 2. Sites of hydrolysis operated by α-chymotrypsin (top, PDB structure: 1ACB) and pepsin (bottom, PDB structure: 4PEP) on RLK10 peptides as predicted by the PeptideCutter online tool [39]. The glycosylation site (asparagine) is highlighted in red. For each enzyme, all the possible fragments obtained from the hydrolysis of the respective sites are shown. (For interpretation of the references to colour in this figure legend, the reader is referred to the Web version of this article.)

Table 2
MIC values (μM) of the RLK10 peptides detected against a panel of *Gram-negative* (*Acinetobacter baumannii* ATCC 17878, *Escherichia coli* ATCC 25922) and *Gram-positive* bacteria (*Staphylococcus aureus* ATCC 6538P and *Listeria monocytogenes* ATCC 7644). As a control, the experiments were also performed with GKY10 peptide.

Peptide	*Escherichia coli* ATCC 25922	*Acinetobacter baumannii* ATCC 17878	*Staphylococcus aureus* ATCC 6538P	*Listeria monocytogenes* ATCC 7644
GKY10	6.25	6.25	6.25	6.25
RLK10	6.25	6.25	6.25	6.25
RLK10-NAG	12.5	50.0	12.5	25.0
Ac-RLK10-NAG	25.0	50.0	25.0	50.0

Table 3
MIC values (μM) of the RLK10 peptides against *Escherichia coli* and *Staphylococcus aureus* untreated (Control) and treated with α-chymotrypsin (100 nM) for 15 min at 37 °C, with pepsin (200 nM) for 60 min at 37 °C, and after incubation in 10 % FBS for 1 h and 24 h at 37 °C.

Pre-treatment with α-chymotrypsin					
Escherichia coli ATCC 25922			*Staphylococcus aureus* ATCC 6538P		
Peptide	Control	Treated	Peptide	Control	Treated
RLK10	6.25	>200	RLK10	6.25	>200
RLK10-NAG	12.5	50	RLK10-NAG	12.5	50
Ac-RLK10-NAG	25	>200	Ac-RLK10-NAG	25	>200
Pre-treatment with pepsin					
***Escherichia coli* ATCC 25922**			***Staphylococcus aureus* ATCC 6538P**		
Peptide	**Control**	**Treated**	**Peptide**	**Control**	**Treated**
RLK10	6.25	>200	RLK10	6.25	>200
RLK10-NAG	12.5	12.5	RLK10-NAG	12.5	12.5
Ac-RLK10-NAG	25	100	Ac-RLK10-NAG	25	100
Pre-treatment with 10 % FBS					
***Escherichia coli* ATCC 25922**			***Staphylococcus aureus* ATCC 6538P**		
Peptide	**Control**	**10 % FBS**		**Peptide**	**Control**	**10 % FBS**	
		1 h	**24 h**			**1 h**	**24 h**
RLK10	6.25	25	200	RLK10	6.25	50	>200
RLK10-NAG	12.5	50	50	RLK10-NAG	12.5	50	50
Ac-RLK10-NAG	25	>200	>200	Ac-RLK10-NAG	25	>200	>200

the presence of the glycosylated peptide. Indeed, the MIC value for RLK10-NAG is 50 μM for both bacterial strains after α-CT treatment, revealing that the presence of NAG can improve the stability of the sequence against proteases by more than 4 times. Intriguingly, the MIC values of the peptides treated with pepsin (Table 3) revealed that RLK10-NAG completely preserves the antimicrobial activity while RLK10 is not stable when treated with this enzyme. Instead, a dramatic decrease in MIC against both bacterial strains was observed for Ac-RLK10-NAG (4-fold compared to the control), even though, unlike RLK10, the antimicrobial activity was not completely suppressed but severely impaired. Finally, the same experiments as described above were performed after incubation in 10 % FBS (Fetal Bovin Serum) for 1 h and 24 h, to verify the impact of the introduced modifications in a more biologically relevant context. The MIC values are collected at the bottom part of Table 3. After 1 h incubation in FBS, all the peptides show higher MIC values against both the bacterial strains tested. In particular, the MIC values against *E. coli* of RLK10 and RLK10-NAG increased four times (to 25 μM and 50 μM, respectively), indicating a partial suppression of their activity. Instead, the acetylated/glycosylated form with its MIC >200 μM resulted in a complete inactive peptide. After 24 h incubation, the MIC value of RLK10 reached the value of 200 μM, highlighting that the peptide antimicrobial potency is severely compromised. Remarkably, the MIC value of RLK-10-NAG remained constant at 50 μM revealing that a marked albeit reduced activity persisted after FBS treatment. A similar scenario was observed for *S. aureus* as well, pointing out the key role played by the sugar moiety in preserving the antimicrobial activity of the peptide.

3.4. Biophysical characterization

The remarkable biological results reported above have prompted an in-depth physicochemical characterization of the interaction process between the peptides and POPE/POPG (7/3 mol/mol) vesicles, which serve as a model of the lipid matrix of the bacterial membrane [42]. The aim was to elucidate the intricate molecular determinants underpinning the mechanism of action of the peptides towards bacterial model membranes and their different susceptibility to enzymatic degradation to rationalize the biological results.

3.5. Determination of partition constants

As described in the introduction, despite the particular mechanism of action of a given peptide (membranotropic or not), a direct interaction with the lipids of the bacterial membrane must take place first [13,14]. Therefore, steady-state fluorescence spectroscopy measurements were performed to determine the mole fraction partition constants (K_x) of the three peptides for LUVs composed of POPE/POPG. The experiments were performed by preparing several samples at constant peptide concentration (7.6 μM) and varying the concentration of lipids from 0 μM to ~1000 μM. Then, the extent of the interaction was followed by monitoring the fluorescence emission (at 344 nm) of the peptides upon excitation at 280 nm. As an example, Fig. 3 depicts the fluorescence emission spectra of RLK10 as function of total lipid concentration. Panel B shows the binding isotherm obtained from the data reported in panel A of the same Figure, and panels C and D show the binding isotherms for RLK10-NAG and Ac-RLK10-NAG, respectively.

As reported in panel A of Fig. 3, the fluorescence emission spectrum of RLK10 in solution was centred at around 356 nm, indicating a complete exposure of the Trp residue to the aqueous environment [43]. At the highest POPE/POPG concentration, a blue shift of λ_{max} of ~12 nm and an increase of the intensity of emission was detected. These observations reveal that the peptide can interact with model membranes while experiencing a more hydrophobic environment characterized by a lower water content. The increase of the intensity can be attributed to the acquisition of a more ordered peptide structure (see also the CD data) where the aromatic residue is partially shielded from the water molecules. This effect disfavours non-radiative deactivation processes (*e.g.*, vibrational relaxation, internal conversion), leading to an increase of the intensity. The same fluorescence behaviour was observed for RLK10-NAG and Ac-RLK10-NAG (Fig. S8), suggesting that the modified peptides are also able to interact with bacterial model membranes. However, the determined K_x-values highlight that the strength of the interaction is not the same for all peptides. In fact, we found that the K_x values are as follows: $(4.1 \pm 0.5)\cdot10^5$ for RLK10, $(2.8 \pm 0.3)\cdot10^5$ for RLK10-NAG, and $(1.5 \pm 0.2)\cdot10^5$ for Ac-RLK10-NAG. Thus, it appears that the presence of the sugar moiety can partially hamper the binding of the peptide to the membrane, providing steric hindrance and finally leading to a decrease of the K_x value. Introducing the acetylation site at the N-terminus of RLK10-NAG caused a further decrease of the affinity. Both results could explain the slightly reduced antibacterial efficacy of RLK10-derived peptides.

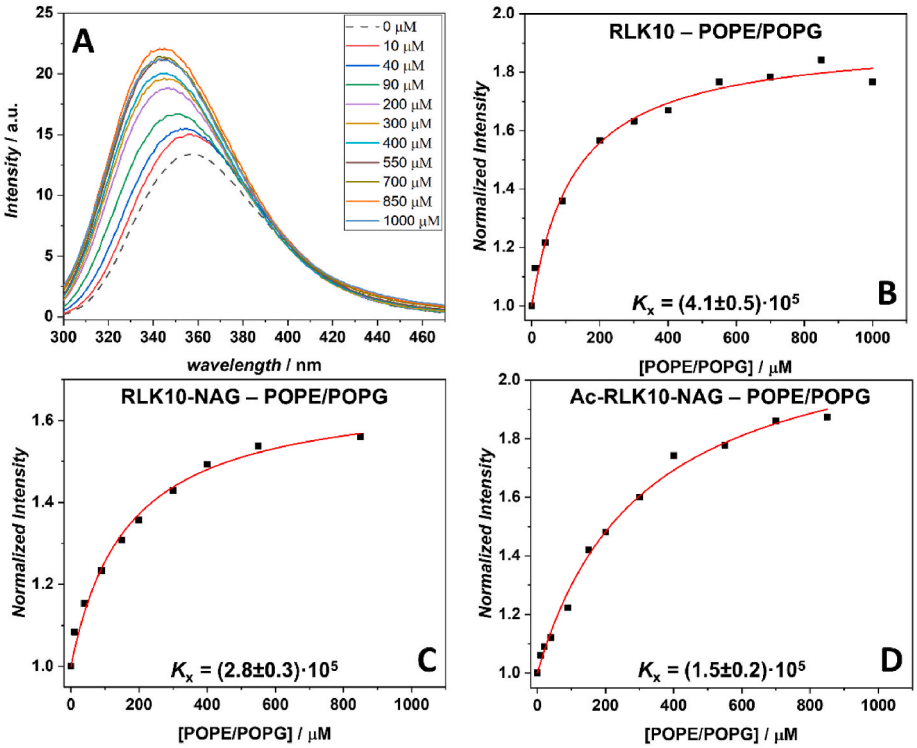

Fig. 3. (A) Fluorescence emission spectra of the RLK10 peptide at the indicated total lipid concentration (LUVs of POPE/POPG 7/3 mol/mol). (B) Binding isotherm obtained from the data reported in panel A. The complex formation was followed at 344 nm upon excitation at 280 nm. Figures (C) and (D) report the binding isotherms obtained from titrations experiments of RLK10-NAG and Ac-RLK10-NAG with LUVs of POPE/POPG, respectively. The red lines in panels B, C and D represent the best fit of experimental data according to the model reported in the Materials and Methods section which allowed the determination of K_x. All the experiments were performed at the temperature of 25 °C in 10 mM sodium phosphate buffer, pH 7.4. (For interpretation of the references to colour in this figure legend, the reader is referred to the Web version of this article.)

3.6. The peptides' conformation upon binding

Circular dichroism (CD) spectroscopy was employed to assess the secondary structure of the peptides in solution and upon binding to the membranes [44]. Fig. 4 depicts the Far-UV CD spectra of RLK10, RLK10-NAG and Ac-RLK10-NAG in neat buffer condition and in the presence of POPE/POPG vesicles.

In neat buffer conditions, all the peptides show a CD spectrum with a minimum around 200 nm, indicating that they adopt an unordered structure. Upon interaction with POPE/POPG vesicles, changes in the CD spectra reveal conformational changes. All the spectra are characterized by two negative bands (at ~205–208 nm and at ~225 nm) and a rising positive one below 200 nm, suggesting the presence of a helical structure. However, the intensities and shapes of the bands are quantitatively different among the peptides. The conformational change imposed by the membrane is most prominent for Ac-RLK10-NAG (which adopts the most ordered structure), followed by RLK10 and then RLK10-NAG. Using the molar ellipticity at 222 nm, the percentages of helical content (H_C) was estimated for all the peptides (inset of Fig. 4). The H_C value for RLK10 in the presence of vesicles is ~27 %. For the glycosylated peptide, the H_C is 16.7 %, indicating that the NAG moiety partially hampers the conformational change. Remarkably, with about 40 % the Ac-RLK10-NAG showed the highest H_C value, *i.e.*, the acetyl group is able to markedly induce and stabilize the helical conformation, as previously shown for some other peptides [36,37]. To better support these findings, the CD spectrum of the acetylated RLK10 (Ac-RLK10) was also recorded (Fig. S9). The reported spectra show that Ac-RLK10 changes its conformation from random coil to a helical one with a H_C value of ~56

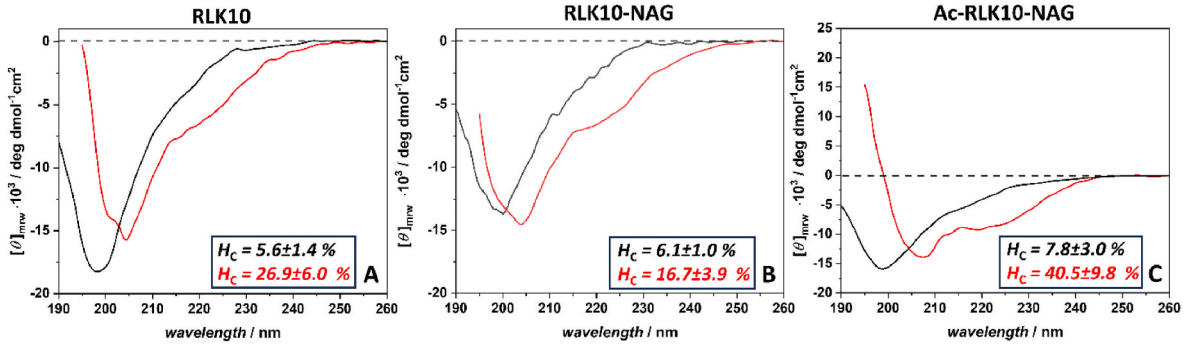

Fig. 4. Far-UV CD spectra of (A) RLK10, (B) RLK10-NAG and (C) Ac-RLK10-NAG in neat buffer (black lines) and in the presence of POPE/POPG LUVs at the lipid-to-peptide ratio of 50. The peptide concentration was 30 μM and the total lipid concentration was 1500 μM. In the insets, the percentage of helical content are shown. All the spectra were recorded in a 0.1 cm path length cuvette at the temperature of 25 °C in 10 mM sodium phosphate buffer, pH 7.4.

%, which is even higher than that of Ac-RLK10-NAG, revealing the high helix-stabilizing effect of the acetyl N-capping group.

3.7. The peptides' perturbation of bacterial model membranes

In the previous paragraphs, the characteristics of the interaction process were studied from the peptide's point of view. To explore also the effects of the peptides on the membrane's mesoscopic and microscopic properties, differential scanning calorimetry (DSC) measurements and fluorescence experiments using the probe Laurdan were carried out. In Fig. 5, panel A, the DSC thermograms of multilamellar vesicles of POPE/POPG in the absence and presence of the peptides RLK10, RLK10-NAG and Ac-RLK10-NAG at the lipid-to-peptide ratio of 10 are collected. The thermodynamics parameters associated to the gel-to-liquid phase transition are reported in Table 4.

The DSC profile of the POPE/POPG vesicles shows a single broad peak, which is due to the gel-to-liquid main phase transition of the lipid bilayer, centred at $T_m = 20.7$ °C and with an associated enthalpy change of 23.9 kJ mol^{-1}, in good agreement with previously reported data [42]. Upon addition of RLK10, no difference in the enthalpy change was observed, indicating that RLK10 is not able to affect the lipid packing of the bilayer significantly. A similar scenario was observed for the glycosylated RLK10-NAG, suggesting that the presence of the sugar moiety does not affect the peptide-membrane interaction. Instead, upon addition of Ac-RLK10-NAG, we observed a dramatic change in the shape of the DSC thermogram. The thermogram is composed of at least two separate peaks, one centred at ~13.6 °C and the other one around 22.6 °C, suggesting peptide-induced domain formation within the lipid bilayer plane. This behaviour can be ascribed to the presence of the acetyl group. Indeed, the DSC thermogram of the POPE/POPG bilayer in the presence of RLK10-NAG does not show such a feature. Further, by performing the same experiment in the presence of the acetylated version of RLK10 (Ac-RLK10), a DSC thermogram (Fig. S10) similar to that of Ac-RLK10-NAG was observed, confirming that it is the acetyl group at the N-terminus of the peptide that induces the lateral phase separation.

Next, using the probe Laurdan, which positions itself at the water–lipid headgroup interface, it is possible to monitor the head group region of the lipid bilayer and the impact of the peptides on disturbing the interfacial region of the lipid bilayer, thus complementing the DSC experiments. The fluorescence emission spectrum of Laurdan informs about the hydration state at the membrane-water interface. Its emission spectrum is characterized by two bands, arising from two emitting states, a non-solvent and a solvent relaxed state. The non-solvent relaxed state emission band appears at ~440 nm and is due to the Laurdan embedded in a less hydrated densely packed lipid state, such as a gel-phase. Instead, the solvent-relaxed state emission band occurs at ~490 nm and is due to Laurdan localized in a more hydrated and less packed liquid-disordered phase. The spectroscopic signature of Laurdan is quantitatively described by means of the general polarization (*GP*) parameter (see the Methods section). Fig. 5, panel B, shows the *GP* values of Laurdan in POPE/POPG unilamellar vesicles as a function of the indicated peptide concentrations. In all cases, an increase of *GP* was observed with increasing peptide concentration, indicating that all peptides dehydrate the membrane interface. Ac-RLK10-NAG has the most prominent effect, which is followed by RLK10 and finally RLK10-NAG.

Table 4
Enthalpy change and temperature for the gel-to-liquid phase transition of POPE/POPG (7/3 mol/mol) multilamellar vesicles in the absence and presence of the indicated peptides at the lipid-to-peptide ratio of 10.

System	[a]ΔH_m/kJ mol^{-1}	T_m/°C
POPE/POPG	23.9 ± 0.6	20.7 ± 0.3
+ RLK10	23.8 ± 0.5	21.1 ± 0.3
+ RLK10-NAG	23.3 ± 0.7	20.3 ± 0.3
+ Ac-RLK10-NAG	23.0 ± 0.8	22.6 ± 0.2

[a] Normalization per total moles of lipids.

3.8. Hydrolysis of the peptides mediated by proteolytic enzymes

The data reported in Table 3 highlight that upon incubation of peptides with the used proteolytic enzymes, the only peptide that still has a significant antimicrobial activity is the glycosylated RLK10-NAG. To rationalize these findings, fluorescence competition kinetic assays were performed, as previously described [26]. Briefly, the enzymes (α-CT at pH 7.4 and pepsin at pH 4.0) were mixed with the fluorescence substrate Ala-Ala-Phe-7-amido-4-methylcoumarin (AAF-AMC) in the absence and in the presence of the RLK10 peptides. Both enzymes are capable of hydrolysing the amide bond between the Phe and AMC, releasing the latter, which can be selectively detected upon excitation at 370 nm and recording the fluorescence emission at 460 nm [38]. In these assays, the peptides act as competitive substrates of AAF-AMC. Thus, if a peptide is preferentially hydrolysed by the enzymes with respect to the fluorescent substrate, the release of AMC from AAF-AMC is retarded. Instead, if a peptide is not hydrolysed at all, a scenario like the control should be observed and the kinetics of the hydrolysis of AAF-AMC in the absence and presence of peptides should be very similar. Of course, intermediate scenarios are possible, depending on the relative affinity of the enzymes for the AAF-AMC and RLK10 peptides.

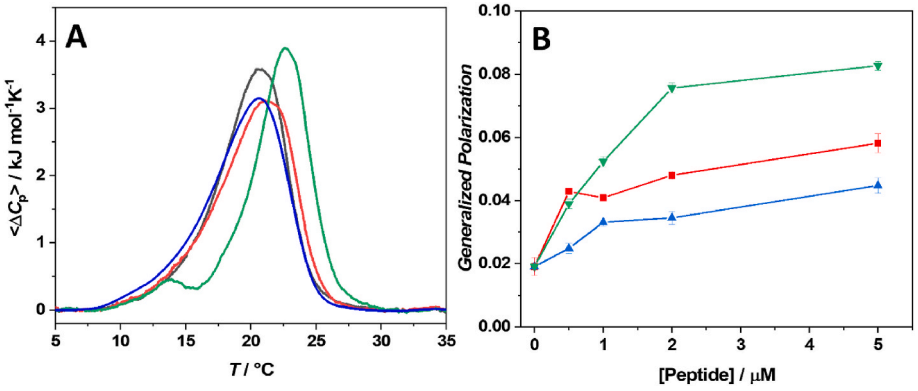

Fig. 5. (A) DSC thermograms of POPE/POPG multilamellar vesicles in the absence (black line) and in the presence of RLK10 (red line), RLK10-NAG (blue line) and, Ac-RLK10-NAG (green line) at the lipid-to-peptide ratio of 10. (B) Generalized polarization of the probe Laurdan embedded in 50 μM POPE/POPG LUVs, at the temperature of 25 °C as a function of peptides concentration: RLK10 (red line), RLK10-NAG (blue line) and Ac-RLK10-NAG (green line). Where not visible, error bars are within the symbol size. All the experiments were performed in 10 mM sodium phosphate buffer, pH 7.4. (For interpretation of the references to colour in this figure legend, the reader is referred to the Web version of this article.)

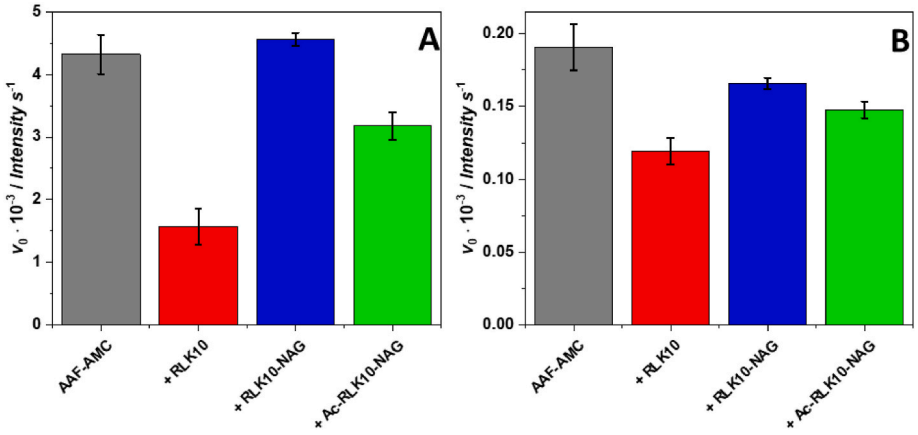

Fig. 6. Bar plots of v_0 for the hydrolysis of the fluorescent substrate AAF-AMC mediated by (A) α-chymotrypsin at pH 7.4 and (B) pepsin at pH 4.0 in the absence and in the presence of RLK10 peptides. All the experiments were performed at the temperature of 25 °C. The error bars are the standard deviations around the average value of v_0 obtained from at least 4 replicates.

Fig. 6 shows the initial rates v_0 (*Intensity* s^{-1}) obtained by evaluating the slope of the linear portion of the fluorescence *Intensity vs. time* plots (Fig. S11).

For α-CT, a reduction of v_0 of about 63 % was observed in the presence of RLK10 compared to the control, indicating that RLK10 is susceptible to the enzyme. Remarkably, for the hydrolysis of AAF-AMC carried out in the presence of RLK10-NAG, the value of v_0 is, within the experimental error, similar to that of the control, revealing successful protection of the peptide by the sugar moiety. Remarkably, for the doubly modified Ac-RLK10-NAG, the v_0 is significantly lower than the control and the value obtained in the presence of RLK10-NAG, suggesting that the acetylation of the free N-terminus does not protect the peptide, but rather enhances peptide susceptibility to enzymatic cleavage. Similar results were obtained for the pepsin, even if the v_0 value obtained in the presence of RLK10-NAG and Ac-RLK10-NAG are only slightly different, being lower for the latter and higher for the former. To strengthen these findings and gain further insights into the cleavage kinetics, the hydrolysis experiments were repeated under similar conditions by incubating the peptides with the two enzymes and monitoring the reactions using RP-HPLC. The obtained chromatograms are collected in Figs. S12 and S13. Instead, the percentages of the recovered intact peptides (evaluated by comparing the areas of the chromatograms' peak) are collected in Table S1. An inspection of Figs. S12–S13 and Table S1 reveals that the hydrolysis of RLK10 operated by α-CT is completed already after 15 min. Instead, for RLK10-NAG and Ac-RLK10-NAG, the percentages of intact peptides were 68 % and 49 %, respectively. For the hydrolysis carried out by pepsin, the percentages of intact peptides after 1 h were 67 %, 98 % and 90 % for RLK10, RLK10-NAG and Ac-RLK10-NAG, respectively. These data, in excellent agreement with those reported in Fig. 6, confirm that RLK10-NAG has the highest resistance to enzymatic hydrolysis followed by Ac-RLK10-NAG and the unmodified RLK10.

4. Discussion

4.1. Effects of the modifications on the action mechanism of RLK10

The short peptide RLK10 showed antimicrobial activity against both *Gram-negative* and *Gram-positive* bacterial strains, like the parent GKY10 peptide. As the latter differs from RLK10 by the substitution of a glutamine with an asparagine residue, these results indicate that the substitution does not affect the peptide's antimicrobial activity as expected, considering the similar structure of these two amino acids. An inspection of Table 2 reveals that the introduction of NAG and the acetyl group alters the antimicrobial activity of the sequence. It was found that the antimicrobial potency of the peptides follows the order RLK10 > RLK10-NAG > Ac-RLK10-NAG. However, the actual activity depends on the modification introduced and, on the bacterium targeted. For example, the MIC value against *E. coli* is two times higher for RLK10-NAG compared to RLK10. Instead, against *A. baumannii*, an 8-times increase of the MIC was observed. For the double-modified form Ac-RLK10-NAG, the MIC-value for *E. coli* is 25 μM, *i.e.* 4 times and 2 times higher than RLK10 and RLK10-NAG, respectively.

These observations prompted a detailed biophysical characterization of the interaction and perturbation of bacterial model membranes mediated by the RLK10 peptides. The obtained values of the partition constants (K_x) clearly indicate that the affinity of the peptides to POPE/POPG LUVs follows the same general order as observed for the MIC values (Table 2). Thus, it seems that the presence of NAG can partially hamper the binding to the membrane, most likely through steric hindrance. Instead, the acetylation at the free N-terminus decreases the affinity for the anionic membrane, likely by reducing the net positive charge of the peptide, a factor generally considered pivotal for the action mechanism and biological activity of AMPs [12]. These results suggest that to overcome the reduction of the bioactivity, one possible strategy is the introduction of an additional modification of the peptide at the C-terminus (*e.g.*, amidation) to preserve the overall peptide charge. Overall, a first difference in the biological activity can be attributed to the different affinities of the peptides for the bacterial model membrane.

Further, it was found that all the peptides change their conformation upon binding, adopting a more ordered helical structure, according to the CD data. The amount of helical content (H_C) follows the order Ac-RLK10-NAG > RLK10 ≥ RLK10-NAG. Interestingly, the peptide Ac-RLK10-NAG with its highest H_C value is the less active, exhibiting the highest MIC-value against all bacterial strains tested. It is widely accepted that most of the linear cationic antimicrobial peptides must adopt a helical conformation upon binding to the membrane to exert their biological function [13,14,45]. However, the relationship between helical content and antimicrobial activity is complex, and cases observing positive, negative and no correlation have been reported. For example, in a study on A12L/A20L, it was found a significant increase of the antibacterial activity against both *Gram-positive* and *Gram-negative* bacteria with an increase of the helical content [46]. Instead, for the LL-37 peptide, a negative correlation was observed, *i.e.* an increase of helical content (prompted by polysorbate 20 and high ionic strength) led to a marked decrease of the antibacterial activity [47]. Finally, on a study on the SJGAP peptide and its variants, no correlation between antibacterial activity and helicity was observed [48]. Our data suggest that in the present case, no correlation exists between conformational change (helix content) and antimicrobial activity, indicating that other

factors play a dominant role.

Differential scanning calorimetry and fluorescence spectroscopy using the Laurdan probe were applied to obtain information on the peptide-induced perturbation of the lipid organization within the bilayer and hydration changes at the level of lipid head groups, respectively. The calorimetric data revealed that RLK10 and RLK10-NAG caused no significant changes in the DSC thermogram of POPE/POPG vesicles. Both, the gel-to-fluid transition temperature and enthalpy change of melting remained essentially unaffected by the presence of peptides, despite the high lipid-to-peptide ratio of 10 used. Thus, it is evident that no marked bilayer perturbation occurred upon binding. In the presence of Ac-RLK10-NAG, the enthalpy change of melting of POPE/POPG vesicles does not change significantly upon peptide interaction, suggesting no perturbation of the hydrophobic core of the bilayer, as seen for the other two peptides. However, a more intricate DSC thermogram was observed. The presence of two separate transitions is evidence that the peptide induces the formation of lipid domains within the lipid bilayer plane. Considering the melting temperature of pure POPE (~ 25 °C) and POPG (~ −5 °C) [42], the lower-melting peak can be attributed to POPG-rich domains and the higher-melting peak to POPE-enriched domains. A similar phenomenon was observed for other peptides, which was attributed to the preferential interaction of the cationic peptide with negatively charged lipids [11, 49], *i.e.*, to strong electrostatic interactions. However, such scenario cannot be the reason in the present case. If just electrostatic interactions drive the lipid segregation process, domain formation should also be observed for RLK10 and RLK10-NAG which possess a higher positive charge compared to the acetylated form. Further, in the case of the Ac-RLK10 peptide (Fig. S10), it is evident that the two well-separated peaks in the DSC thermogram of POPE/POPG are due to the acetyl group. A possible explanation can be found in the ability of the acetyl to provide an additional oxygen capable of forming hydrogen bonds with the lipid head groups (OH for PGs and NH_3^+ for PEs) which, in conjunction with electrostatic interactions, can prompt the formation of domains. Such explanation would be in line with the *GP*-value of Laurdan (Fig. 5, B). Indeed, although RLK10 and RLK10-NAG have higher K_x values compared to Ac-RLK10-NAG, the latter shows higher *GP*-values. This indicates a greater dehydration of the membrane surface induced by Ac-RLK10-NAG suggesting that it mainly acts at the level of the headgroup region. In contrast, the lower *GP* values observed for RLK10, and RLK10-NAG reveal that they are less effective at dehydrating this portion of the membrane. Taken together, DSC and Laurdan experiments reveal marked differences in the modes of action among the peptides. Apparently, the peptides RLK10 and RLK10-NAG do not appear to perturb the membrane. Instead, they may interact with the membrane without inducing permanent damage, allowing them to translocate across the lipid bilayer. Once on the cytosolic side, the peptides could engage with intracellular targets, such as nucleic acids, as reported for some AMPs [12]. The variations in their antimicrobial activity can be attributed to their differing affinities for the membrane, which is higher for RLK10. In contrast, Ac-RLK10-NAG may act through a lipid segregation mechanism where domain formation is prompted by the acetyl group. Domain formation alters the membrane's lateral organization and fluidity, affecting protein sorting and function and ultimately compromising membrane functionality [50]. This mechanism involves high-energy costs associated with lipid redistribution and reorganization and may be less effective compared to that of the other two peptides. Additionally, Ac-RLK10-NAG exhibits the lowest affinity for the bacterial model membrane. Taken together, these two factors may explain the strongly reduced biological activity of this variant.

4.2. *Effects of the modifications on the stability of RLK10 in serum and against enzymatic degradation*

As stated in the introduction section, the application of AMPs is limited by their poor stability, particularly against enzymes capable of hydrolysing the amide bonds, leading to peptide fragmentation and their inactivation. To enhance the stability of RLK10 peptide, two modifications were introduced. In RLK10-NAG, N-acetylglucosamine (NAG) was covalently attached to the asparagine residue. Instead, Ac-RLK10-NAG was obtained by acetylating the N-terminus of RLK10-NAG. The stability against proteases was assessed against the enzymes α-chymotrypsin and pepsin both *in cellulo* and *in vitro*. The data presented in Table 3 indicate that treatment of RLK10 and Ac-RLK10-NAG with α-CT completely inactivated both sequences. Similar results were observed after treating RLK10 with pepsin. However, complete inactivation was not seen for Ac-RLK10-NAG despite a significant compromise in biological activity. Notably, pretreatment with α-CT only slightly affected the biological activity of RLK10-NAG, and no changes with respect to the control were noted after treatment with pepsin. Collectively, these findings demonstrate that the presence of the sugar moiety renders the sequence less susceptible to the proteases' action. Interestingly, introducing a small acetyl group into RLK10-NAG markedly affects its resistance.

To rationalize these findings, we conducted *in vitro* experiments in two ways: by means of fluorescence kinetics assay (Fig. 6) and RP-HPLC (Figs. S12 and S13). The two set of data are in excellent agreement with each other. As shown in Fig. 2, α-CT hydrolyses the peptides at two sites. The bond next to the Trp is very close to the glycosylated site. Thus, the presence of the sugar may partially hamper the recognition of this site by the enzyme. The other hydrolysis site is next to the Leu residue. At its N-terminus, there are an Arg and the N-terminal free amino group that carries a positive charge at pH 7.4. Its acetylation removes this charge while increasing the hydrophobic character of this portion of the peptide, thus favouring binding in the hydrophobic pocket of the enzyme compared to the non-acetylated peptides. The enzyme pepsin can hydrolyze the peptide bond next to residue 4 (Lys). This site is not too far from the glycosylation site. Hence, the presence of NAG could disfavour the binding of the enzyme similar to α-chymotrypsin, explaining the data reported in Table 3 and Fig. 6, S12 and S13. When RLK10-NAG is acetylated, a reduced antimicrobial activity was detected after pepsin treatment, in agreement with the data shown in Fig. 6, S12 and S13. Thus, the introduction of the acetyl group renders the peptide more susceptible to protease action, possibly due to enhanced enzyme binding facilitated by hydrogen bond formation with some residues in the active site and/or increased hydrophobic character of this peptide portion, which may favor its localization in the pepsin's active site. Of note, the data obtained by means of RP-HPLC (Figs. S12 and S13 and Table S1) suggest that the observed biological activities of the modified forms are due to their incomplete cleavage rather than a full resistance to the proteases. Indeed, after the treatment of RLK10-NAG with α-CT (15 min incubation), the recovered intact peptide is 68 % of its initial amount. The MIC value obtained after α-CT treatment is 4 times higher compared to the untreated peptide. Thus, the reduced antimicrobial potency is due to incomplete cleavage, or in other words, the presence of NAG slows down the hydrolysis of the amide bonds. The comparison of the data obtained with the unmodified RLK10 reveals a further piece of information. Indeed, the partially preserved bioactivity of RLK10-NAG may also be due to the production of active fragments. However, this does not appear to be the case. Indeed, the hydrolysis sites are the same for all the peptides. Consequentially, if the fragments were bioactive, a residual activity of RLK10 should also be observed. Similar conclusions can be invoked for Ac-RLK10-NAG. However, after α-CT treatment, this peptide is basically inactive. This phenomenon can be explained considering that the amount of intact peptide after α-CT treatment is 49 %, well below the amount detected for RLK10-NAG. Thus, the concentration of active Ac-RLK10-NAG is strongly reduced, that in conjunction with its lower antimicrobial potency compared to RLK10-NAG explain the observed antimicrobial properties (Table 3). The same explanation can be applied to the peptides treated with pepsin, reinforcing our conclusions. Finally, the resistance of the three peptides was also tested after incubation in serum (Table 3). The data showed that after 1 h, the MIC

values against *E. coli* of RLK10 and RLK10-NAG increased 4 times compared to the controls. Instead, Ac-RLK10-NAG with its MIC >200 μM is inactivated. Surprisingly, after 24 h also RLK10 was inactivated. Instead, RLK10-NAG preserved its antimicrobial potency having a MIC value similar to that observed after 1 h. Similar results were observed also against *S. aureus* highlighting that the sole presence of the NAG moiety is crucial in preserving the activity of the peptide. It is important to note that the serum is a complex mixture of proteins, lipids and carbohydrates (and other smaller molecules). The inactivation of RLK10 and Ac-RLK10-NAG can be due to proteases action present in the serum and to the interaction with some serum components (*e.g.,* albumin) that led to the decrease of the amount of free peptide capable to exert the antimicrobial activity. Instead, for RLK10-NAG it seems that the decrease of activity is due to the interaction with serum components only. Indeed, if proteases against it are active, the MIC value should increase after 24 h as observed for the other two peptides. This observation is in line with the observed data described above. Collectively, the reported data show that the only presence of NAG covalently linked to the Asn residue is effective in protecting the sequence from proteolytic degradation and possibly hampering the interaction of the peptide with serum components.

5. Conclusions

In this study, the peptide RLK10 was synthesized starting from the short version of the thrombin-derived peptide GKY10 and subjected to two modifications: glycosylation at the asparagine residue and acetylation at the free N-terminus. These modifications aimed to improve its stability while also promoting helical propensity - a factor considered critical for determining the antimicrobial activity of linear cationic AMPs. The introduction of N-acetylglucosamine was demonstrated to significantly enhance the stability of the RLK10 sequence against proteases and in serum, while only marginally affecting its biological activity compared to the parent peptide. Unexpectedly, further modification through acetylation did not improve the peptide resistance, rather it increased its susceptibility to degradation, possibly in serum as well. Moreover, although the presence of the acetyl group rendered the peptide more prone to adopt a helical structure, it resulted in a significant reduction of the bioactivity.

Biophysical data collectively provide insights into the possible causes behind these observed differences, which can be attributed to varying modes of action and differing affinities for the bacterial membrane. The peptides RLK10 and RLK10-NAG appear to act in a similar way by interacting with the lipid bilayer without causing detectable membrane damage. Upon binding, these peptides may translocate across the membrane reaching the intracellular space and targeting various intracellular components. In contrast, Ac-RLK10-NAG induces the formation of lipid domains that may be less effective regarding translocation and its subsequent biological effects.

In conclusion, we met our goal of producing a peptide that hold the best combination in terms of antimicrobial activity and resistance to proteases, by simply introducing a glycosylated Asn into a short peptide. Increasing the stability of AMPs without significantly altering their biological activity remains a primary focus in peptide research, facilitating their application in medicine as new antibiotics and extending their use into areas such as food preservation and biotechnology.

CRediT authorship contribution statement

Ilaria Di Donato: Writing – review & editing, Investigation. **Attila Tortorella:** Writing – review & editing, Investigation, Data curation. **Marco Campanile:** Writing – review & editing, Investigation. **Andreas Rumpel:** Writing – review & editing, Investigation, Data curation. **Linda Leone:** Writing – review & editing, Investigation. **Andrea Bosso:** Writing – review & editing, Investigation, Data curation. **Luigi Petraccone:** Writing – review & editing, Methodology. **Angelina Lombardi:** Writing – review & editing, Supervision, Methodology, Funding acquisition. **Roland Winter:** Writing – review & editing, Methodology, Funding acquisition. **Pompea Del Vecchio:** Writing – review & editing, Writing – original draft, Supervision, Funding acquisition, Conceptualization. **Rosario Oliva:** Writing – review & editing, Writing – original draft, Visualization, Supervision, Methodology, Funding acquisition, Formal analysis, Data curation, Conceptualization.

Declaration of competing interest

The authors declare that they have no known competing financial interests or personal relationships that could have appeared to influence the work reported in this paper.

Acknowledgments

R.W. acknowledges funding from the Deutsche Forschungsgemeinschaft (DFG, German Research Foundation) under Germany's Excellence Strategy – EXC 2033 – project number 390677874-RESOLV. R.O. acknowledges "Programma per il Finanziamento della Ricerca di Ateneo (FRA) 2022" from University of Naples Federico II for the financial support. P.D.V. acknowledges PRIN_2022 (Project BELIEVE_ Biomimetic antimicrobial vesicle-like nanoarchitectures for multi-drug-resistant bacteria, Project number: 2022HSFEPY, CUP: E53D2300840006). The authors acknowledge the Italian MUR program "Dipartimenti di Eccellenza 2023–2027" for the project arCHIMede [CUP E63C22003710006]. This study was carried out within the Agritech National Research Center and received funding from the European Union Next-GenerationEU (PIANO NAZIONALE DI RIPRESA E RESILIENZA (PNRR) – MISSIONE 4 COMPONENTE 2, INVESTIMENTO 1.4 – D.D. 1032 June 17, 2022, CN00000022). This manuscript reflects only the authors' views and opinions, neither the European Union nor the European Commission can be considered responsible for them.

Appendix A. Supplementary data

Supplementary data to this article can be found online at https://doi.org/10.1016/j.abb.2025.110526.

Data availability

Data will be made available on request.

References

[1] https://www.who.int/news-room/fact-sheets/detail/antimicrobial-resistance.
[2] M.K. Byrne, S. Miellet, A. McGlinn, J. Fish, S. Meedya, N. Reynolds, A.M. van Oijen, The drivers of antibiotic use and misuse: the development and investigation of a theory driven community measure, BMC Public Health 19 (2019) 1425, https://doi.org/10.1186/s12889-019-7796-8.
[3] Samreen, I. Ahmad, H.A. Malak, H.H. Abulreesh, Environmental antimicrobial resistance and its drivers: a potential threat to public health, J. Glob. Antimicrob. Resist. 27 (2021) 101–111, https://doi.org/10.1016/j.jgar.2021.08.001.
[4] G. Kapoor, S. Saigal, A. Elongavan, Action and resistance mechanisms of antibiotics: a guide for clinicians, J. Anaesthesiol. Clin. Pharmacol. 33 (2017) 300–305, https://doi.org/10.4103/joacp.JOACP_349_15.
[5] E. Peterson, P. Kaur, Antibiotic resistance mechanisms in bacteria: relationships between resistance determinants of antibiotic producers, environmental bacteria, and clinical pathogens, Front. Microbiol. 9 (2018), https://doi.org/10.3389/fmicb.2018.02928.
[6] M.N. Alekshun, S.B. Levy, Molecular mechanisms of antibacterial multidrug resistance, Cell 128 (2007) 1037–1050, https://doi.org/10.1016/j.cell.2007.03.004.
[7] E. Arad, K.B. Pedersen, O. Malka, S. Mambram Kunnath, N. Golan, P. Aibinder, B. Schiøtt, H. Rapaport, M. Landau, R. Jelinek, Staphylococcus aureus functional amyloids catalyze degradation of β-lactam antibiotics, Nat. Commun. 14 (2023) 8198, https://doi.org/10.1038/s41467-023-43624-1.
[8] A. Bahar, D. Ren, Antimicrobial peptides, Pharmaceuticals 6 (2013) 1543–1575, https://doi.org/10.3390/ph6121543.
[9] P. Kumar, J. Kizhakkedathu, S. Straus, Antimicrobial peptides: diversity, mechanism of action and strategies to improve the activity and biocompatibility in vivo, Biomolecules 8 (2018) 4, https://doi.org/10.3390/biom8010004.

[10] M.N. Melo, R. Ferre, M.A.R.B. Castanho, Antimicrobial peptides: linking partition, activity and high membrane-bound concentrations, Nat. Rev. Microbiol. 7 (2009) 245–250, https://doi.org/10.1038/nrmicro2095.
[11] V. Teixeira, M.J. Feio, M. Bastos, Role of lipids in the interaction of antimicrobial peptides with membranes, Prog. Lipid Res. 51 (2012) 149–177, https://doi.org/10.1016/j.plipres.2011.12.005.
[12] C.-F. Le, C.-M. Fang, S.D. Sekaran, Intracellular targeting mechanisms by antimicrobial peptides, Antimicrob. Agents Chemother. 61 (2017) e02340, https://doi.org/10.1128/AAC.02340-16, 16.
[13] J. Lei, L. Sun, S. Huang, C. Zhu, P. Li, J. He, V. Mackey, D.H. Coy, Q. He, The antimicrobial peptides and their potential clinical applications, Am. J. Transl. Res. 11 (2019) 3919–3931.
[14] A.J. Alanis, Resistance to antibiotics: are we in the post-antibiotic era? Arch. Med. Res. 36 (2005) 697–705, https://doi.org/10.1016/j.arcmed.2005.06.009.
[15] M. Campanile, R. Oliva, P.D. Vecchio, R. Winter, L. Petraccone, The anticancer peptide LL-III binds with nanomolar affinity to human telomeric and cMyc G-quadruplexes, Chem. Commun. 59 (2023) 6179–6182, https://doi.org/10.1039/D3CC00737E.
[16] R. Oliva, S.K. Mukherjee, L. Ostermeier, L.A. Pazurek, S. Kriegler, V. Bader, D. Prumbaum, S. Raunser, K.F. Winklhofer, J. Tatzelt, R. Winter, Remodeling of the fibrillation pathway of α-Synuclein by interaction with antimicrobial peptide LL-III, Chem. Eur J. 27 (2021) 11845–11851, https://doi.org/10.1002/chem.202101592.
[17] M. Campanile, E.D. Kurtul, R. Dec, S. Möbitz, P. Del Vecchio, L. Petraccone, J. Tatzelt, R. Oliva, R. Winter, Morphological transformations of SARS-CoV-2 nucleocapsid protein biocondensates mediated by antimicrobial peptides, Chem. Eur J. 30 (2024) e202400048, https://doi.org/10.1002/chem.202400048.
[18] R.K. Thapa, D.B. Diep, H.H. Tønnesen, Topical antimicrobial peptide formulations for wound healing: current developments and future prospects, Acta Biomater. 103 (2020) 52–67, https://doi.org/10.1016/j.actbio.2019.12.025.
[19] R. Oliva, M. Chino, K. Pane, V. Pistorio, A. De Santis, E. Pizzo, G. D'Errico, V. Pavone, A. Lombardi, P. Del Vecchio, E. Notomista, F. Nastri, L. Petraccone, Exploring the role of unnatural amino acids in antimicrobial peptides, Sci. Rep. 8 (2018) 8888, https://doi.org/10.1038/s41598-018-27231-5.
[20] K.E. Greber, M. Dawgul, Antimicrobial peptides under clinical trials, Curr. Top. Med. Chem. 17 (2017) 620–628, https://doi.org/10.2174/1568026616666160713143331.
[21] V. Cafaro, A. Bosso, I. Di Nardo, A. D'Amato, I. Izzo, F. De Riccardis, M. Siepi, R. Culurciello, N. D'Urzo, E. Chiarot, A. Torre, E. Pizzo, M. Merola, E. Notomista, The antimicrobial, antibiofilm and anti-inflammatory activities of P13#1, a cathelicidin-like achiral peptoid, Pharmaceuticals 16 (2023) 1386, https://doi.org/10.3390/ph16101386.
[22] E. Grimsey, D.W.P. Collis, R. Mikut, K. Hilpert, The effect of lipidation and glycosylation on short cationic antimicrobial peptides, Biochim. Biophys. Acta - Biomembr. 1862 (2020) 183195, https://doi.org/10.1016/j.bbamem.2020.183195.
[23] R. Oliva, F. Battista, S. Cozzolino, E. Notomista, R. Winter, P. Del Vecchio, L. Petraccone, Encapsulating properties of sulfobutylether-β-cyclodextrin toward a thrombin-derived antimicrobial peptide, J. Therm. Anal. Calorim. 138 (2019) 3249–3256, https://doi.org/10.1007/s10973-019-08609-7.
[24] N.G. Bednarska, B.W. Wren, S.J. Willcocks, The importance of the glycosylation of antimicrobial peptides: natural and synthetic approaches, Drug Discov. Today 22 (2017) 919–926, https://doi.org/10.1016/j.drudis.2017.02.001.
[25] J.A. Mackintosh, D.A. Veal, A.J. Beattie, A.A. Gooley, Isolation from an ant Myrmecia gulosa of two inducible O-Glycosylated proline-rich antibacterial peptides, J. Biol. Chem. 273 (1998) 6139–6143, https://doi.org/10.1074/jbc.273.11.6139.
[26] A. Tortorella, L. Leone, A. Lombardi, E. Pizzo, A. Bosso, R. Winter, L. Petraccone, P. Del Vecchio, R. Oliva, The impact of N-glycosylation on the properties of the antimicrobial peptide LL-III, Sci. Rep. 13 (2023) 3733, https://doi.org/10.1038/s41598-023-29984-0.
[27] R. Oliva, M. Campanile, P.D. Vecchio, E. Pizzo, A. Bosso, R. Winter, L. Petraccone, The C-terminus of the GKY20 antimicrobial peptide, derived from human thrombin, plays a key role in its membrane perturbation capability, Phys. Chem. Chem. Phys. 24 (2022) 7994–8002, https://doi.org/10.1039/D1CP05857F.
[28] R. Oliva, P. Del Vecchio, M.I. Stellato, A.M. D'Ursi, G. D'Errico, L. Paduano, L. Petraccone, A thermodynamic signature of lipid segregation in biomembranes induced by a short peptide derived from glycoprotein gp36 of feline immunodeficiency virus, Biochim. Biophys. Acta - Biomembr. 1848 (2015) 510–517, https://doi.org/10.1016/j.bbamem.2014.10.017.
[29] A. Chakrabartty, T. Kortemme, R.L. Baldwin, Helix propensities of the amino acids measured in alanine-based peptides without helix-stabilizing side-chain interactions, Protein Sci. 3 (1994) 843–852, https://doi.org/10.1002/pro.5560030514.
[30] A.S. Ladokhin, S. Jayasinghe, S.H. White, How to measure and analyze Tryptophan Fluorescence in membranes properly, and why bother? Anal. Biochem. 285 (2000) 235–245, https://doi.org/10.1006/abio.2000.4773.
[31] T. Parasassi, E.K. Krasnowska, L. Bagatolli, E. Gratton, Laurdan and prodan as polarity-sensitive fluorescent membrane probes, J. Fluoresc. 8 (1998) 365–373, https://doi.org/10.1023/A:1020528716621.
[32] L. Ostermeier, R. Oliva, R. Winter, The multifaceted effects of DMSO and high hydrostatic pressure on the kinetic constants of hydrolysis reactions catalyzed by α-chymotrypsin, Phys. Chem. Chem. Phys. 22 (2020) 16325–16333, https://doi.org/10.1039/D0CP03062G.
[33] Pepsin - Worthington enzyme manual | Worthington Biochemical, (n.d.). https://www.worthington-biochem.com/products/pepsin/manual (accessed March 19, 2025).
[34] E. Lampitella, N. Landi, R. Oliva, R. Gaglione, A. Bosso, F. De Lise, S. Ragucci, A. Arciello, L. Petraccone, E. Pizzo, P. Del Vecchio, A. Di Maro, Toxicity and membrane perturbation properties of the ribotoxin-like protein Ageritin, J. Biochem. 170 (2021) 473–482, https://doi.org/10.1093/jb/mvab062.
[35] R. Oliva, P.D. Vecchio, A. Grimaldi, E. Notomista, V. Cafaro, K. Pane, V. Schuabb, R. Winter, L. Petraccone, Membrane disintegration by the antimicrobial peptide (P)GKY20: lipid segregation and domain formation, Phys. Chem. Chem. Phys. 21 (2019) 3989–3998, https://doi.org/10.1039/C8CP06280C.
[36] X. Wang, S.C. Moore, M. Laszckzak, J. Ausió, Acetylation increases the α-Helical content of the histone tails of the nucleosome, J. Biol. Chem. 275 (2000) 35013–35020, https://doi.org/10.1074/jbc.M004998200.
[37] J. Brango-Vanegas, M.L. Leite, M.L.R. Macedo, M.H. Cardoso, O.L. Franco, Capping motifs in antimicrobial peptides and their relevance for improved biological activities, Front. Chem. 12 (2024), https://doi.org/10.3389/fchem.2024.1382954.
[38] R. Oliva, S. Banerjee, H. Cinar, R. Winter, Modulation of enzymatic activity by aqueous two-phase systems and pressure – rivalry between kinetic constants, Chem. Comm. 56 (2020) 395–398, https://doi.org/10.1039/C9CC08065A.
[39] E. Gasteiger, C. Hoogland, A. Gattiker, S. Duvaud, M.R. Wilkins, R.D. Appel, A. Bairoch, Protein identification and analysis tools on the ExPASy server, in: J. M. Walker (Ed.), The Proteomics Protocols Handbook, Humana Press, Totowa, NJ, 2005, pp. 571–607, https://doi.org/10.1385/1-59259-890-0:571.
[40] Y. Hamuro, S.J. Coales, K.S. Molnar, S.J. Tuske, J.A. Morrow, Specificity of immobilized porcine pepsin in H/D exchange compatible conditions, Rapid Commun. Mass Spectrom. 22 (2008) 1041–1046, https://doi.org/10.1002/rcm.3467.
[41] D.L. Nelson, M.M. Cox, A.A. Hoskins, Lehninger Principles of Biochemistry, (n.d.) 4381.
[42] B. Pozo Navas, K. Lohner, G. Deutsch, E. Sevcsik, K.A. Riske, R. Dimova, P. Garidel, G. Pabst, Composition dependence of vesicle morphology and mixing properties in a bacterial model membrane system, Biochim. Biophys. Acta - Biomembr. 1716 (2005) 40–48, https://doi.org/10.1016/j.bbamem.2005.08.003.
[43] J.T. Vivian, P.R. Callis, Mechanisms of Tryptophan fluorescence shifts in proteins, Biophys. J. 80 (2001) 2093–2109, https://doi.org/10.1016/S0006-3495(01)76183-8.
[44] S.M. Kelly, T.J. Jess, N.C. Price, How to study proteins by circular dichroism, Biochim. Biophys. Acta, Proteins Proteomics 1751 (2005) 119–139, https://doi.org/10.1016/j.bbapap.2005.06.005.
[45] J. Koehbach, D.J. Craik, The vast structural diversity of antimicrobial peptides, Trends Pharmacol. Sci. 40 (2019) 517–528, https://doi.org/10.1016/j.tips.2019.04.012.
[46] Y. Huang, L. He, G. Li, N. Zhai, H. Jiang, Y. Chen, Role of helicity of α-helical antimicrobial peptides to improve specificity, Protein Cell 5 (2014) 631–642, https://doi.org/10.1007/s13238-014-0061-0.
[47] D.O. Ulaeto, C.J. Morris, M.A. Fox, M. Gumbleton, K. Beck, Destabilization of α-Helical structure in solution improves bactericidal activity of antimicrobial peptides: opposite effects on bacterial and viral targets, Antimicrob. Agents Chemother. 60 (2016) 1984–1991, https://doi.org/10.1128/aac.02146-15.
[48] S. Cashman-Kadri, P. Lagüe, I. Fliss, L. Beaulieu, Determination of the relationships between the chemical structure and antimicrobial activity of a GAPDH-Related fish antimicrobial peptide and analogs thereof, Antibiotics 11 (2022) 297, https://doi.org/10.3390/antibiotics11030297.
[49] T.-H. Lee, V. Hofferek, F. Separovic, G.E. Reid, M.-I. Aguilar, The role of bacterial lipid diversity and membrane properties in modulating antimicrobial peptide activity and drug resistance, Curr. Opin. Chem. Biol. 52 (2019) 85–92, https://doi.org/10.1016/j.cbpa.2019.05.025.
[50] H. Khandelia, J.H. Ipsen, O.G. Mouritsen, The impact of peptides on lipid membranes, Biochim. Biophys. Acta - Biomembr. 1778 (2008) 1528–1536, https://doi.org/10.1016/j.bbamem.2008.02.009.